Composites: Part A 161 (2022) 107121

Contents lists available at ScienceDirect

Composites Part A

journal homepage: www.elsevier.com/locate/compositesa

Rapid and energy-efficient manufacturing of thermoset prepreg via localized in-plane thermal assist (LITA) technique

Kaiyue Deng [a], Chunyan Zhang [b], Xiangyang Dong [c,*], Kun Kelvin Fu [a,d,*]

[a] Department of Mechanical Engineering, University of Delaware, Newark, DE 19716, USA
[b] Department of Materials Science and Engineering, University of Delaware, Newark, DE 19716, USA
[c] Department of Mechanical and Aerospace Engineering, Missouri University of Science and Technology, Rolla, MO 65409, USA
[d] Center for Composite Materials, University of Delaware, Newark, DE 19716, USA

ARTICLE INFO

Keywords:
Prepreg
Thermosetting resin
Resin flow
Capillary effect

ABSTRACT

Prepregs are in demand for large production by the composites manufacturing industry to improve the mechanical properties of the load-bearing structural parts. The current prepreg manufacturing is confronted with inadequate resin impregnation, high energy costs, and safety concerns. To address those challenges, in this paper, we proposed a novel thermoset prepreg fabrication strategy that utilizes viscosity controlled by thermal gradient as well as gravity to achieve fast and energy-efficient manufacturing of thermoset prepreg. The concept is based on the localized in-plane thermal assist (LITA) technique, which uses a dynamic capillary effect to induce the wicking of thermoset resins in carbon fibers. This work demonstrated that a bench-scale continuous production of thermoset prepreg with carbon fiber tows can be achieved, and results show that the produced prepreg is B-staged, with the degree of curing as 13.9%. Our calculation suggests that the LITA prepreg fabrication method could save 63.56% of energy compared to the traditional prepreg fabrication methods, and increase the production rate by 133.28% compared to the traditional hot-melt prepreg fabrication method. The LITA prepreg method represents an efficient and eco-friendly composite manufacturing technology to outperform the state-of-the-art energy-intensive prepreg fabrication methods.

1. Introduction

Carbon fiber/thermoset composites are strong and lightweight materials that have been widely used in the aerospace, automotive, and wind energy industries [1–5]. In composites manufacturing, prepregs are applied in the large structural parts due to their high fiber volume fraction (65%) [6] and ease of moldability, so they are ready to be used as intermediate materials through a layer-by-layer stacking way to form predetermined patterns for large-volume composite structure production. The shape conformity of a prepreg allows it to be laid up to the surface of tooling structure closely and fully cured into the final composite structural parts by post-thermal curing [1,7]. Prepregs consist of fibers and thermoset resins (e.g., epoxy, vinyl ester, and phenolic resin) that are slightly cured (often known as B-staging), and the fabrication is implemented by liquid thermoset infiltration into the fiber. Because of the very low curing degree (<35%) [8–10] of resin in prepreg, prepreg can be saved for long-term use if it is properly stored at low temperature to retard polymer cross-linking kinetics. Driven by the ambitious global target of achieving zero Green House Gases (GHG) emission by 2050 [11–13], prepreg demand for making lightweight and strong composite has been largely increased, particularly in sustainable energy applications, such as weight-efficient ground and flying vehicles, electric vehicle battery enclosure, pressure vessels for hydrogen, and turbine blades for wind energy. In order to meet the energy-saving goals, it requires the high-volume and massive carbon fiber/thermoset prepreg production to be more energy-efficient and environmentally friendly.

Prepreg production is a liquid thermoset resin impregnation while maintaining a low degree of resin curing process. Traditionally, thermoset resin impregnation is plagued by poor impregnation rate, limited choices of suitable thermoset resin, high energy costs, and safety concerns. To solve those challenges, three common solutions are adopted, including the solvent dip method, the hot-melt method and the resin filming method to form prepregs [14–16]. In the solvent dip method, fiber tows are usually soaked in a resin bath containing resins and

* Corresponding authors at: Department of Mechanical and Aerospace Engineering, Missouri University of Science and Technology, Rolla, MO 65409, USA (X. Dong). Department of Mechanical Engineering, University of Delaware, Newark, DE 19716, USA (K. K. Fu).
E-mail addresses: dongxi@mst.edu (X. Dong), kfu@udel.edu (K.K. Fu).

https://doi.org/10.1016/j.compositesa.2022.107121
Received 4 May 2022; Received in revised form 11 July 2022; Accepted 26 July 2022
Available online 30 July 2022
1359-835X/© 2022 Elsevier Ltd. All rights reserved.

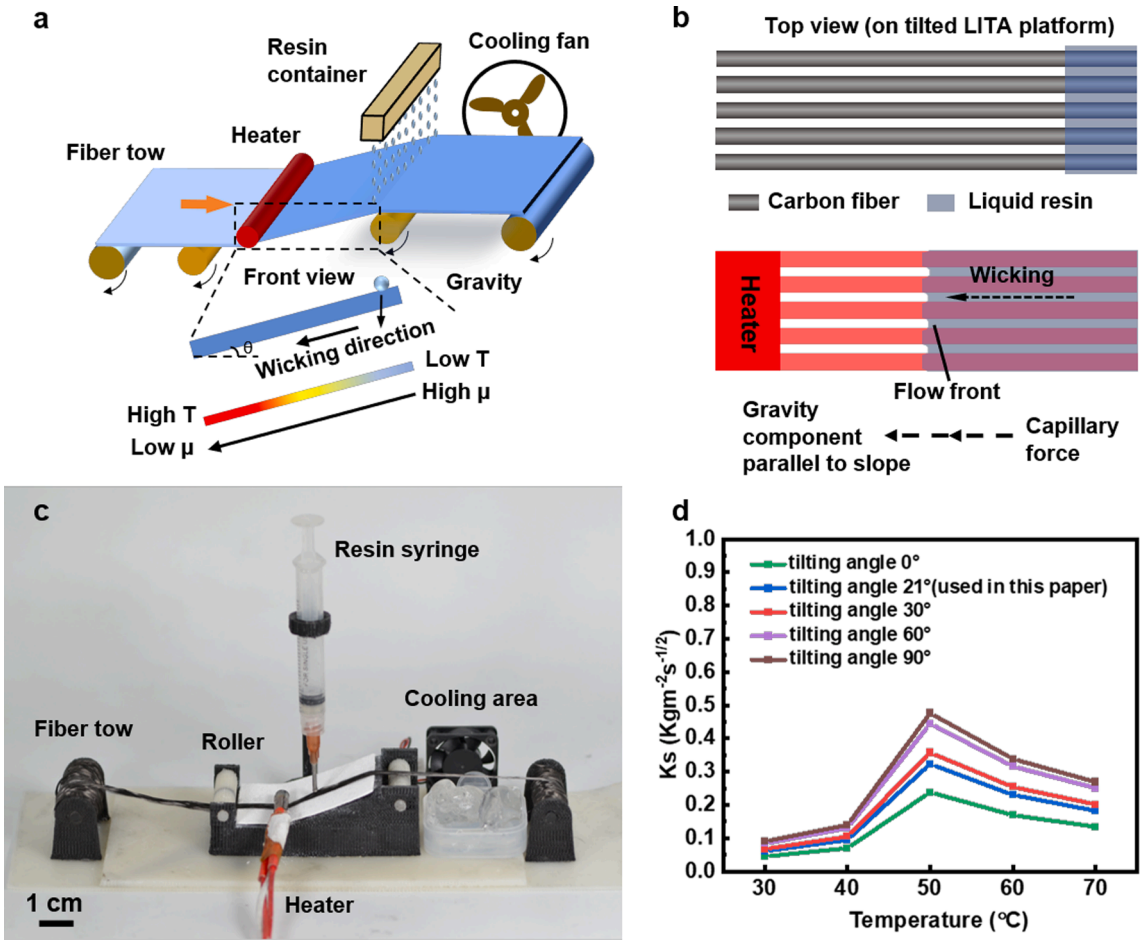

Fig. 1. Illustration of the LITA thermoset prepregs fabrication process. (a) Schematic of the prepregs fabrication process. The heater, which is situated 10 mm away from the resin droplets, contacts the moving fiber tow on the sloped conveyor, leading to a thermal gradient for the resin droplets to infiltrate to the fiber. The gravity also helps resin flow towards the lower end of the slope, where the heater is placed. The cooling area helps ensure B-staging of the prepregs. (b) Top view of the carbon fiber tows, where the capillary effect takes place with heater and gravity driving the resin flow front. (c) Digital photo of the bench-scale continuous prepregs production system. (d) Liquid sorption coefficient K_s of the resin vs temperature and tilting angle, with the highest values occurring at 50 °C for all tilting angles. (For interpretation of the references to colour in this figure legend, the reader is referred to the web version of this article.)

organic solvents, where organic solvents (e.g., acetone, ethyl acetate, methyl ethyl ketone) are used to reduce the viscosity of the resin to facilitate fast resin impregnation into carbon fiber structures [8,17,18]. Once the resin is fully saturated in the prepreg, organic solvents need to be removed from the prepregs in the air circulation oven [18]. The organic solvent removal and reclaim process will deteriorate impregnation with voids left by solvent removal, and potentially cause safety concerns and raise energy costs [14]. The organic solvents are avoided in the hot-melt method. In this method, the resin flows from the hopper to the release paper with heat applied to drop the viscosity, and transfers to the fiber by rolling. Then, the resin-carried release paper is calendared with the fiber to enforce impregnation. However, the calendaring rollers must be also heated to maintain the low viscosity of the resin, due to the possibility of heat dissipation between the resin hopper and the rollers. Not only the rollers consumes energy during operation, but also the prolonged heating on the thermosets enhances the degree of crosslinking and gradually increases viscosity, thus it degrades the impregnation sufficiency [14,15]. The resin filming method uses similar equipment as the hot melt method, but uses the resin film that has been pre-manufactured to limit contact with heat to only calendaring. However, the resin film could have poor flexibility and high viscosity due to raw materials and B-staging, so it is also challenging to achieve full impregnation [15,16]. Recent efforts are made to improve the thermoset prepreg fabrication processes, including the radio-frequency (RF) assisted prepreg fabrication method [19], the siphon prepreg fabrication method [20], and the T-Die prepreg fabrication method [21]. In the RF assisted prepreg fabrication method, the RF applicator was introduced to replace the conventionally used oven to saturate the fiber with the resin. The RF applicator could better control the crosslinking of the carbon fiber/epoxy prepreg with predefined power and heating time. The optimized frequency was found to be 66 MHz to obtain the maximized heating rate at low power input, which enables fast fabrication of the prepregs with low energy consumption. However, this method did not consider solvent recollection before applying the electromagnetic wave. The evaporation of the remaining solvent on the fiber under high heating rate makes the process not comply with safety requirements [19]. In the siphon method, the fiber was feeding through the siphon, where the amount of resin could be adjusted by hydrostatic pressure to control the impregnation rate. However, the syphon is not suitable for high-viscosity resins, as it has high requirements for the flowability of the resin and the flexibility of the prepreg to adapt to the curvature of the siphon [20]. The T-Die method was to improve the hot-melt prepreg method by replacing the calendaring rollers to the T-die, which concentrates the heating area to promote impregnation, but the tooling and energy costs are high [21]. An ideal prepreg fabrication method should meet several following traits: (1) no organic solvent, (2) possess high thermoset impregnation rate, (3) be adaptable for all types of thermoset matrices, (4) do not require high energy consumption. However,

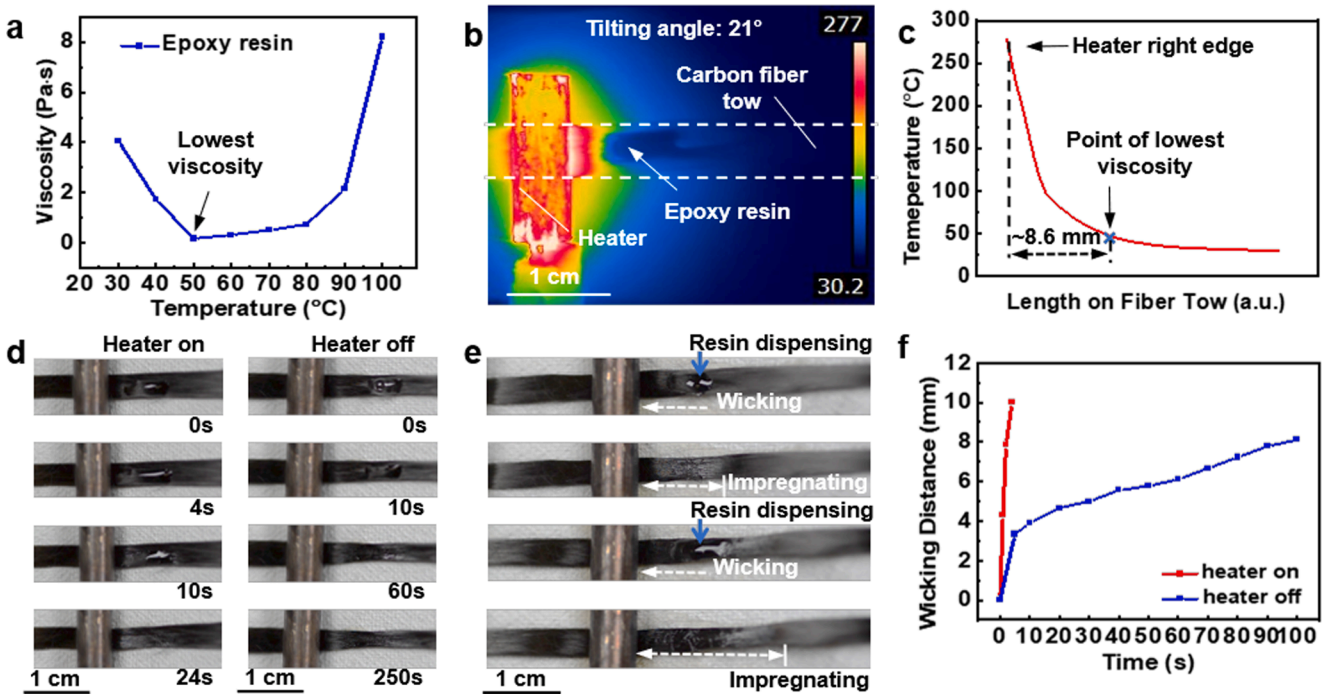

Fig. 2. Demonstration of the LITA prepreg fabrication process using epoxy resin on fiber tows. (a) Viscosity vs temperature (30 ~ 100 °C, with 10 °C as an interval) for the epoxy resin (FibreGlast System 4600, curing agent System 4690. The weight ratio of resin to curing agent is 5:1). (b) Infrared (IR) image of temperature distribution on 12 K carbon fiber tow (HexTow, Hexcel Corporation, Stamford, CT) during epoxy resin wicking on LITA platform (tilting angle 21°), recorded in FLIR camera. (c) Plot of temperature distribution along fiber direction. (d) Top view photos of epoxy resin wicking to form the prepreg (Left: with heating is applied. Right: without heating.). (e) Top view photos of continuous wicking with heating applied. (f) Wicking distance vs time on the bench-scale prepreg system with heating applied and without heating. (For interpretation of the references to colour in this figure legend, the reader is referred to the web version of this article.)

currently reported methods only have touched part of those traits, while our fabrication method addresses all of those traits.

In this work, we propose a novel thermoset prepreg fabrication method that is solvent-free, efficient in thermoset impregnation, applicable for a wide range of thermoset resins and energy-saving. The core mechanism of the fabrication method is the localized in-plane thermal assist (LITA) technique, with dynamic capillary effect of the resin caused by thermal gradient to realize fast resin impregnation on the fiber and maintain B-staging of the resin matrix with low energy costs. We recently developed a 3D printer based on the LITA mechanism [22]. The schematic of the LITA thermoset prepreg fabrication method is shown in Fig. 1, where a bench-scale continuous production system is established for thermoset prepregs with carbon fiber tows. A heater is utilized to preheat carbon fibers and induce a temperature gradient along the fiber feeding direction. With resin deposited on fibers, the temperature gradient creates the viscosity gradient of the resin, which presents the opposite trend as the temperature gradient in the vicinity of the heater. The variation of temperature-dependent viscosity facilitates wicking phenomenon on carbon fibers. The correlation between viscosity and wicking phenomenon could be indicated using the liquid sorption coefficient of the epoxy resin that had been introduced in our previous LITA work. In that previous work, we developed the equation of liquid sorption coefficient K_s, which measures the wicking capability of resin on carbon fibers that had capillary effect on the horizontal plane [22]. In this work, the slope of the LITA conveyor assists in resin wicking by gravity, together with capillary effect. Based on this, we introduced the coefficient $(1+\sin\alpha)$ to the K_s to represent the coupling effects of gravity and capillary force, and formed the equation for the modified liquid sorption coefficient K_s^m as shown in equation (1). We also plotted curves of the K_s^m to reveal the trend of temperature-dependent wicking capability in Fig. 1(d), where the highest K_s^m values occur at 50 °C for all tilting angles. This modified equation is not an accurate physics representation. It is just to reflect the coupling effects of capillary force and gravity on resin wicking and impregnation qualitatively.

The impregnated fiber tows need cooling to suppress cross-linking of the infiltrated resin. With cooling area placed before the collection spool of the fabricated prepregs, the fiber cools down to 12.5 ~ 18.2 °C tested with IR camera. The temperature is appropriate to inhibit the cross-linking, and prolong the storage life. The curing kinetics of the prepregs are inhibited by the cooling area, accordingly the B-staging is maintained after resin impregnation. The produced prepregs turn out to achieve a low degree of curing, as 13.9%, which is in the percentage range of B-staging. By comparing with conventional prepreg [23–26] and other production [27,28] we can confirm the competitiveness of the LITA prepreg method with its production rate 133.28% higher than the hot-melt prepreg fabrication method and its energy intensity 63.56% lower than the traditional prepreg fabrication methods, which stands out our method as an efficient and eco-friendly composite manufacturing technology.

$$K_s^m = K_s(1+sin\alpha) = \left[d_1\sqrt{\frac{\gamma}{\mu}}\right]\left[\sqrt{\frac{\varepsilon^*}{\lambda}}\sqrt{r_0}\right]\left[\sqrt{\frac{cos\theta}{2}}\right](1+sin\alpha)$$

(1, adapted from [22])

K_s is the liquid sorption coefficient, and K_s^m is the modified liquid sorption coefficient. d_1 is the density of the resin, γ is the surface tension of the resin, μ is the viscosity of the resin, ε^* is the effective sorption porosity of carbon fiber tows, λ is the tortuosity factor which can be calculated using geometric relations between carbon fibers and pores. r_0 is the average pore radius, θ is the contact angle between resin and fiber tows, and α is the tilting angle of the LITA conveyor. The equation of K_s and values of surface tension, effective sorption porosity, tortuosity factor, average pore radius, contact angle are referenced from previous work in LITA [22].

The LITA prepreg fabrication process has been experimentally demonstrated. The temperature-dependent viscosity profile in Fig. 2(a) shows a dramatically decreasing trend from 30 to 50 °C and a slightly

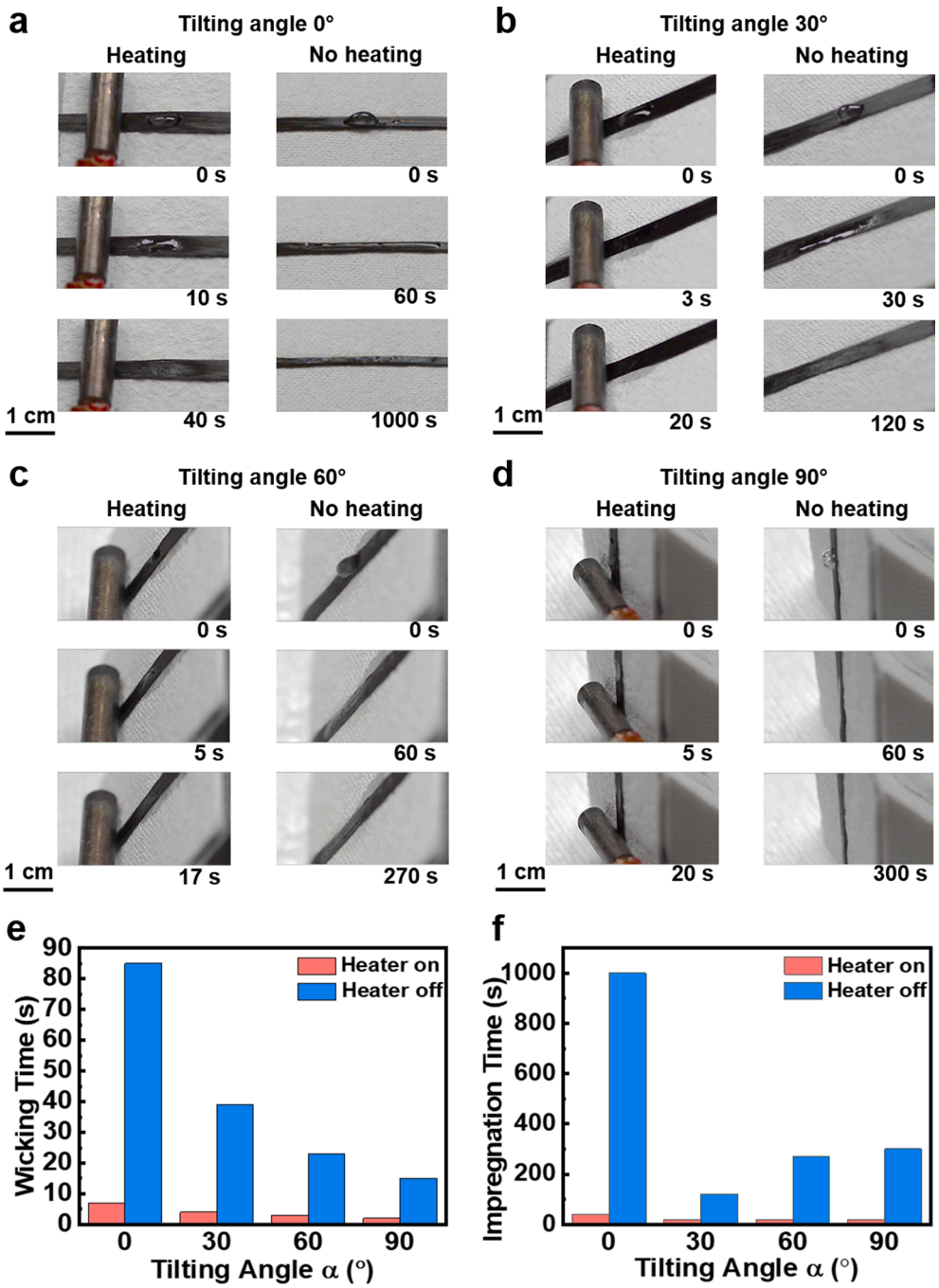

Fig. 3. Demonstration of tilting-induced wicking on 12 K carbon fiber tows. (a) Resin impregnation on fiber tows which are placed 0°. (b) Resin impregnation on fiber tows which are placed 30°. (c) Resin impregnation on fiber tows which are placed 60°. (d) Resin impregnation on fiber tows which are placed 90°. (e) Wicking time vs slope degree with heating applied to the fibers and without heating. (f) Impregnation time vs slope degree with heating applied and without heating. (For interpretation of the references to colour in this figure legend, the reader is referred to the web version of this article.)

increasing trend between 50 and 80 °C. The resin viscosity dramatically increases when the temperature is over 90 °C. The lower bound of viscosity occurs at 50 °C, with a value of 0.156 Pa·s. As for the epoxy resin that we used in the experiments, it has lowest viscosity and highest liquid sorption coefficient at 50℃. This temperature should be considered as the best temperature to preheat the resin. At the specific deposition spot, the temperature of resin can be lower than the temperature of the deposition spot, so as to keep temperature to the same during LITA operation. But the preheating temperature beyond the deposition spot would oppositely create obstacle for resin flowing and infiltration. The infrared (IR) image in Fig. 2(b) shows a temperature distribution along fiber tow, with a temperature range of 30.2 °C ~ 277 °C, as the heater is closely contacting the carbon fibers. The temperature distribution is correspondingly graphed in Fig. 2(c), which indicates that the temperature is ~ 42.1 °C at the point of resin deposition, which is ~ 8.6 mm away from the right edge of heater. Fig. 2(d) presents the dynamic wicking of resin on fiber tow over time by digital photos. The resin deposited on fiber tow is a mixture of an epoxy resin (FibreGlast System 4600, Brookville, OH, USA) and a hardener (FibreGlast 4690) by the weight ratio of 5:1. The heater was operated at 1.0A 10.0 V using Keithley 2425 source meter, with the output power as 6.68 W on the left side of Fig. 2(d). The resin deposited on fiber tow reacted immediately to the thermal gradient, and spread over the wicking region within 5 s by capillary force as well as gravity. By 40 s, it was observed that the resin was almost absorbed into fibers. The right side of the figure presents much slower wicking and impregnation performances of the resin without heating. Although the wicking could also occur in 10 s only by gravity, the resin could not be seen fully absorbed into the fiber until 250 s. The continuous wicking process with heating applied is demonstrated in Fig. 2(e) by digital photos. The continuous resin deposition on

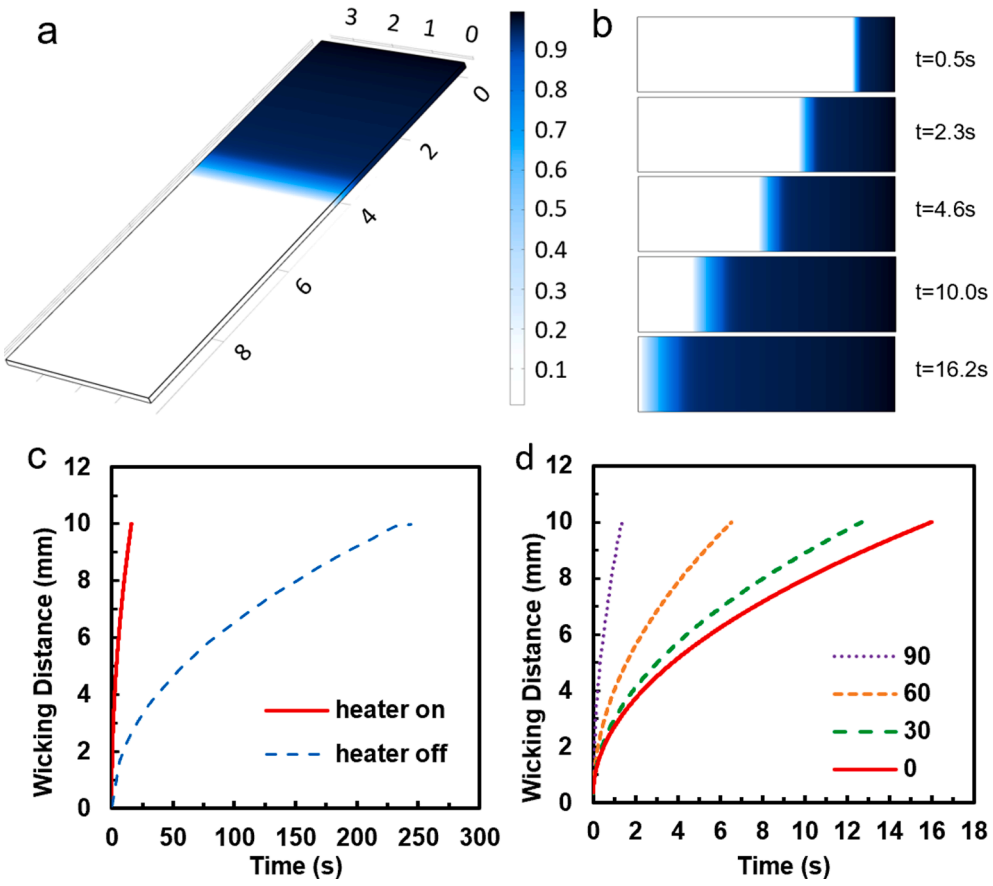

Fig. 4. Predictive modeling of the resin wicking process with regards to applied fiber heating and varied conveyor slope for the LITA prepreg fabrication method. (a) Schematic of fiber tow and resin wicking simulation setup (the unit is mm), with (b) showing top view of the representative percentage of resin absorbed by the fiber tow at different times with applied fiber heating at a conveyor slope of 0°. (c) The effect of applied fiber heating on wicking distance over time. (d) The effect of gravity on wicking distance over time, as controlled by the slope degree of the conveyor. (For interpretation of the references to colour in this figure legend, the reader is referred to the web version of this article.)

two different spots followed by wicking and impregnation, and constitutes a new longitudinal wicking region on the fiber driven by capillary force and gravity, which seamlessly covers fiber tow with continuous resins. Fig. 2(f) illustrates the wicking distance of resin on fiber tow with a small amount of resin used. The resin wicking reaches 10 mm at ~ 4 s with heating applied to the fibers, while the resin only approaches ~ 4.7 mm at 20 s without heating. Different resin systems may have different lower bound of viscosity, highest liquid sorption coefficient and corresponding temperature. As for the epoxy resin that we used in the experiments, it has lowest viscosity and highest liquid sorption coefficient at 50 ℃. This temperature should be considered as the best temperature to preheat the resin. At the specific deposition spot, the temperature of resin can be lower than the temperature of the deposition spot, so as to keep temperature to the same during LITA operation. But the preheating temperature beyond the deposition spot would oppositely create obstacle for resin flowing and infiltration.

To study the role of applied fiber heating and varied conveyor slope on the proposed prepreg fabrication method, we prepared LITA prepreg miniature production lines at different tilting angles from 0 to 90°, with 30°as an interval. The digital photos of resin wicking are shown in Fig. 3 (a)-(d) at the various tilting angles. The left-side sub-photos are with heater working at 280 ℃, and the right-side sub-photos are without heating. In Fig. 3(a), the resin at tilting angle as 0°wicked towards the heater within 10 s, and infiltrated into fibers within 40 s with heating applied; without heat, the resin took the longest time as 1000 s to complete infiltration. In Fig. 3(b), with tilting angle as 30°, the resin wicked within 3 s, and infiltrated within 20 s; even without heat, the resin only needed 30 s to wick, and 120 s to infiltrate. In Fig. 3(c), the resin wicked within 5 s, and completed impregnation within 17 s with heating applied at tilting angle as 60°; without heat, the resin wicked within 60 s, and infiltrated within 270 s. In Fig. 3(d), at tilting angle as 90°, the resin still wicked within 5 s, and infiltrated within 20 s with heating applied; without heat, the resin completed wicking within 60 s, and impregnation within 300 s. The wicking and impregnation time of the experimented tilting angles are summarized in Fig. 3(e) and 3(f), respectively. Each plot contains the time recorded with heating applied (1.0A 10.0 V, output power ≈ 6.53 W), and without heating. When the wicking of the resin stalls on fiber tow, it was observed that the volume of the resin shrank down on fiber surface, and the resin was being absorbed into carbon fiber structures. The time presented both in the two column figures was recorded starting from when the resin was deposited onto fiber tow. According to the results, the wicking time is inversely proportional to the degree of tilting, which works for both with heat applied and without heat. As for the impregnation time, it is similar at 30, 60 and 90°, and higher at 0°with heating applied; but the impregnation time is higher at 60 and 90°than low degree of tilting when the heat is not applied. At 30°, it has the lowest impregnation time as 120 s. It can be attributed that at high degree of tilting, the lower stream of fiber tows has more resin accumulated, where it needs more time to infiltrate into fibers. Generally, the wicking time and the impregnation time of resin on fiber with heat applied are significantly shorter than those without heat. Considering the fact that the resin initial attachment onto carbon fibers becomes difficulty as titling angle increases that makes resin roll over, which will cause an unsaturated scenario of carbon fibers through the thickness, our experimental shows that 20-30° tilting angles can have the best wicking/impregnation time and resin saturation performance.

To better understand the role of applied fiber heating and varied conveyor slope on the proposed prepreg fabrication method, we also implement a wicking model here in COMSOL Multiphysics to analyze the resin wicking process shown in Fig. 4. The predictive model of the resin wicking on the fiber tow is set up as a 2D model of a fiber tow with a rectangular geometry of 10 mm length (referred to the wicking distance between the resin droplet and the heater) and 3.6 mm width

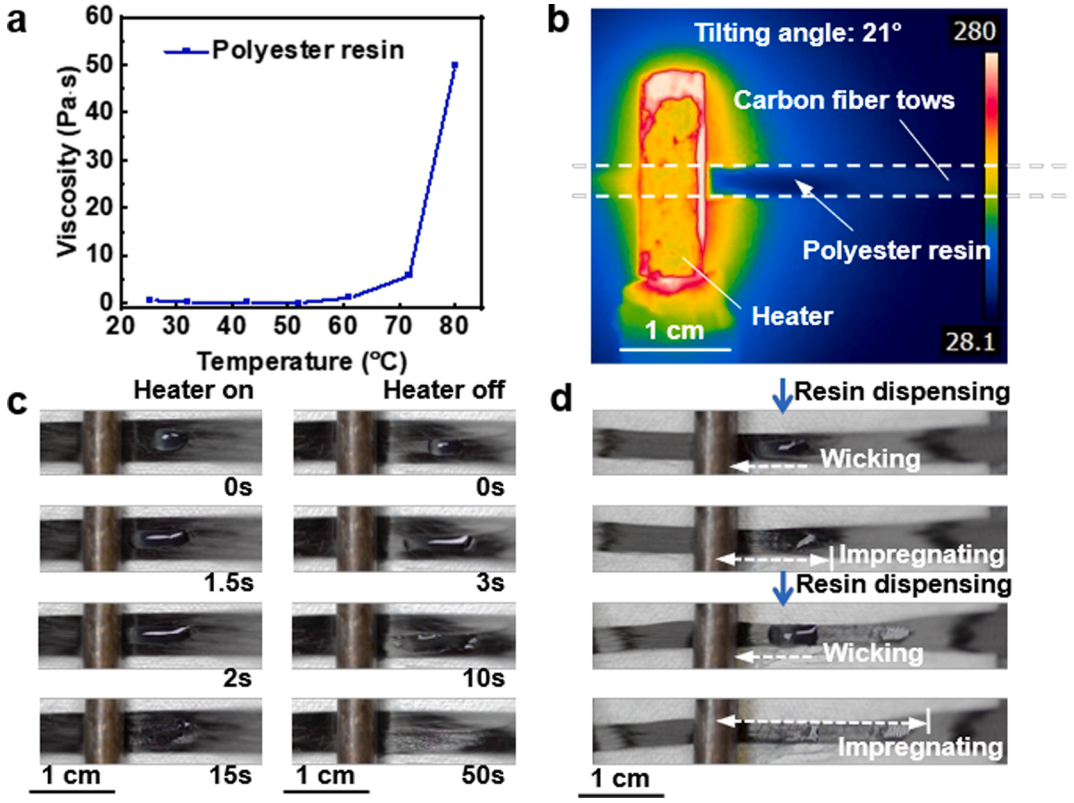

Fig. 5. LITA demonstration of polyester resin on 12 K carbon fiber tows. (a) Viscosity of polyester resin vs temperature, in the range of 25 ~ 80 ℃. (b) Infrared (IR) image of temperature distribution (recorded in FLIR camera) on 12 K carbon fiber tow (HexTow, Hexcel Corporation, Stamford, CT), which was placed on LITA platform (tilting angle: 21°) for polyester resin wicking. (polyester resin: TotalBoat Polyester Laminating Resin Marine Grade) (c) Top view photos of resin to form prepreg (Left: with heating is applied (1.0A, 10 V, output ≈6.68 W). Right: without heating.) on the 12 K carbon fiber tow (HexTow, Hexcel Corporation, Stamford, CT). (d) Top view photos of continuous wicking with heating applied (1.0A, 10 V, output ≈ 6.68 W). (For interpretation of the references to colour in this figure legend, the reader is referred to the web version of this article.)

(estimated from the fiber tow used in this study) in Fig. 4(a). A thickness of 0.12 mm is also defined based on the measured fiber tow thickness. It is worth noting that while a 1-D analytical solution could be used here, we develop the 2D model in this study to account for potential temperature (thus wicking) variation along the fiber tow width for comparison in the follow-up study, e.g., carbon fiber fabrics. In comparison, the Multiphysics analysis models the resin wicking as a multiphase flow by coupling the Darcy's law and phase transport in porous media. The effective porosity and average pore radius are calculated to be 0.465 and 1.29 μm, respectively, for the fiber tow in this study. A thermal gradient is applied along the fiber tow length, following the experimentally measured temperature distribution in Fig. 2(c) in order to predict wicking process along fiber length. The corresponding experimentally measured temperature dependent resin viscosity in Fig. 2(f), surface tension and contact angle characterized in our previous study [22] are implemented to explicitly study fiber heating effect here. A uniform temperature distribution is only applied across fiber tow cross-section (i.e., fiber tow width and thickness) in the 2D model here to simplify the simulation process. A transient simulation of wicking a fiber tow length of 10 mm is performed, with representative resin wicking levels at different times shown in Fig. 4(b). The resin starts infusing the fiber tow very quickly at initial stages, and then gradually slows down as it approaches the total fiber length. Similar phenomena are also observed from both experimental results in Fig. 2 and prediction results in Fig. 4. The effect of the proposed fiber heating is first analyzed in Fig. 4(c). Similar to the experimental measurement in Fig. 2(g), fiber heating decreases the time needed to infuse fiber tow from above 260 s to 16 s, dramatically improving the wicking rate. The effect of gravity on resin flowing is studied by varying slope degrees in Fig. 4(d). Increasing the slope degree from 0° to 90° is also found to greatly reduce the time needed from 16 s to 1.7 s in wicking the fiber tow length of 10 mm in Fig. 4(d). It is worth noting that as only the slope degree is changed, it will only affect resin flowing (wicking) rate and thus the predicted trend is expected to be self-similar with only varying slope as observed in Fig. 4(d). It should also be noted that the discrepancies found between experimental measurements in Fig. 2 and prediction results Fig. 4 are mainly attributed to the difference in temperature distribution through fiber thickness, where a uniform temperature distribution is applied along fiber thickness in the 2D model here. However, in our experiments, the contact-based fiber heating method may cause temperature gradient through fiber thickness, leading to both wicking along fiber length in Fig. 2(h) and absorption through fiber thickness in Fig. 2(i).

To validate the capability of LITA method on other resin system, we have demonstrated the feasibility of polyester resin on fiber tows. The viscosity profile of the polyester resin is shown in Fig. 5(a). The viscosity is 0.713 Pa•s at 25 ℃, and decreases to lowest value as 0.138 Pa•s at 52 ℃. Beyond this temperature, the viscosity significantly rises. Fig. 5(b) shows the temperature distribution on fiber tows with polyester resin. The temperature of the lowest viscosity of resin determines the location of deposition spot for the polyester resin, which is ~ 10 mm away from the right edge of the heater. The digital photos of deposition of polyester resin droplets are shown in Fig. 5(c). With heating applied, the resin infiltrated into fiber tows within 15 s, while the resin took 50 s to infiltrate. Fig. 5(d) shows the continuous wicking of polyester resin on fiber tows with heater maintaining at 280 ℃. The demonstration proves the potential to expand the method to other resin systems.

Besides the test of other resin system, we also have demonstrated the feasibility of the LITA method on woven fabrics with epoxy and polyester resins. The IR image in Fig. 6(a) shows the temperature distribution along the woven fabrics during the epoxy resin wicking in the range of

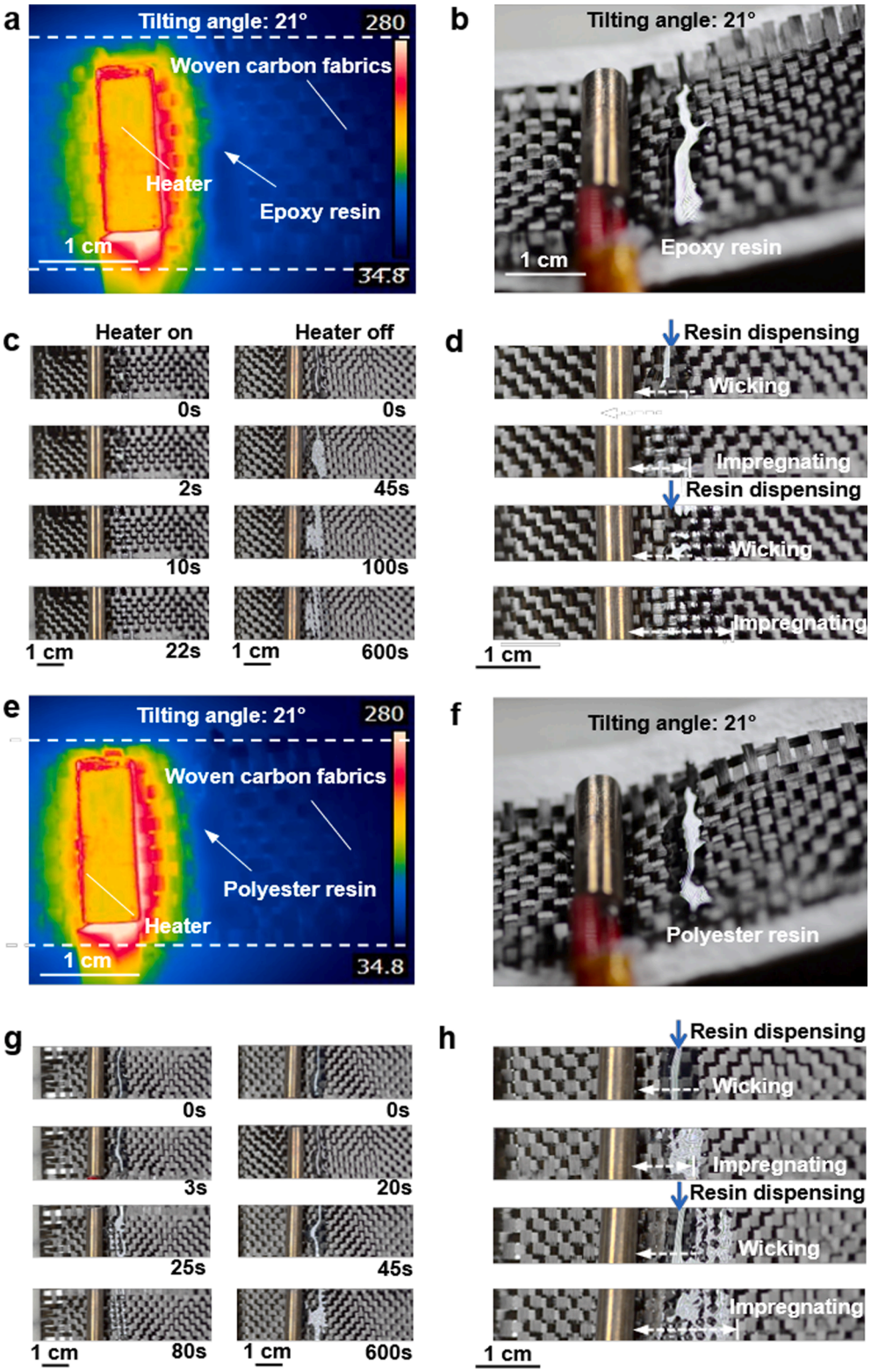

Fig. 6. LITA demonstration of epoxy resin and polyester resins on woven carbon fabrics. (a)-(d): Epoxy resin. (a) Infrared (IR) image (recorded in FLIR camera) of temperature distribution on woven carbon fabrics during wicking of epoxy resin), which was placed on LITA platform (tilting angle: 21°). (epoxy resin: FibreGlast System 4600 mixed with the hardener System 4690 in the weight ratio of 5:1). (b) Side view photo of epoxy resin wicking at the same time as taking the IR image. (c) Top view photos of epoxy resin wicking to form prepreg (Left: with heating is applied (1.0A, 10 V, output ≈6.68 W). Right: without heating.) on the 3 K woven fabrics (BONT Carbon fiber cloth fabric sheet, plain weave 3 K). (d) Top view photos of continuous wicking with heating applied (1.0A, 10 V, output ≈6.68 W). (e)-(h): Polyester resin. (e) Infrared (IR) image (recorded in FLIR camera) of temperature distribution on woven carbon fabrics during wicking of polyester resin on LITA platform (tilting angle: 21°), recorded in FLIR camera. (polyester resin: TotalBoat Polyester Laminating Resin Marine Grade). (f) Side view photo of polyester resin wicking at the same time as taking the IR image. (c) Top view photos of polyester resin wicking to form prepreg (Left: with heating is applied (1.0A, 10 V, output ≈6.68 W). Right: without heating.) on the 3 K woven fabrics. (d) Top view photos of continuous wicking with heating applied (1.0A, 10 V, output ≈6.68 W). (For interpretation of the references to colour in this figure legend, the reader is referred to the web version of this article.)

34.8 ~ 280 ℃. Combined with viscosity data in Fig. 2(a) and the temperature distribution in Fig. 6(a), we deposited the epoxy resin on woven fabrics ~ 8.1 mm away from the right edge of the heater. Fig. 6(b) shows the simultaneous digital photo of resin wicking as the IR image. Fig. 6(c) displays the dynamic wicking of epoxy resin on woven fabrics. The left images in Fig. 6(a) show that with heat applied on the woven fabrics, the epoxy resin was infiltrated into the woven fabrics within 22 s, while it took the resin 600 s to be infiltrated to the woven fabrics without heat shown in the right images of Fig. 6(c). Fig. 6(d) displays the continuous resin wicking of the epoxy resin with heat applied, with temperature of heater reaching ~ 280 ℃. The experiments demonstrate that the woven fabrics can also be used in LITA method for the resin to be infiltrated with thermal gradient from the adjacent heater. Fig. 6(e)-(h) are regarding polyester resin, deposited on woven fabrics ~ mm away from

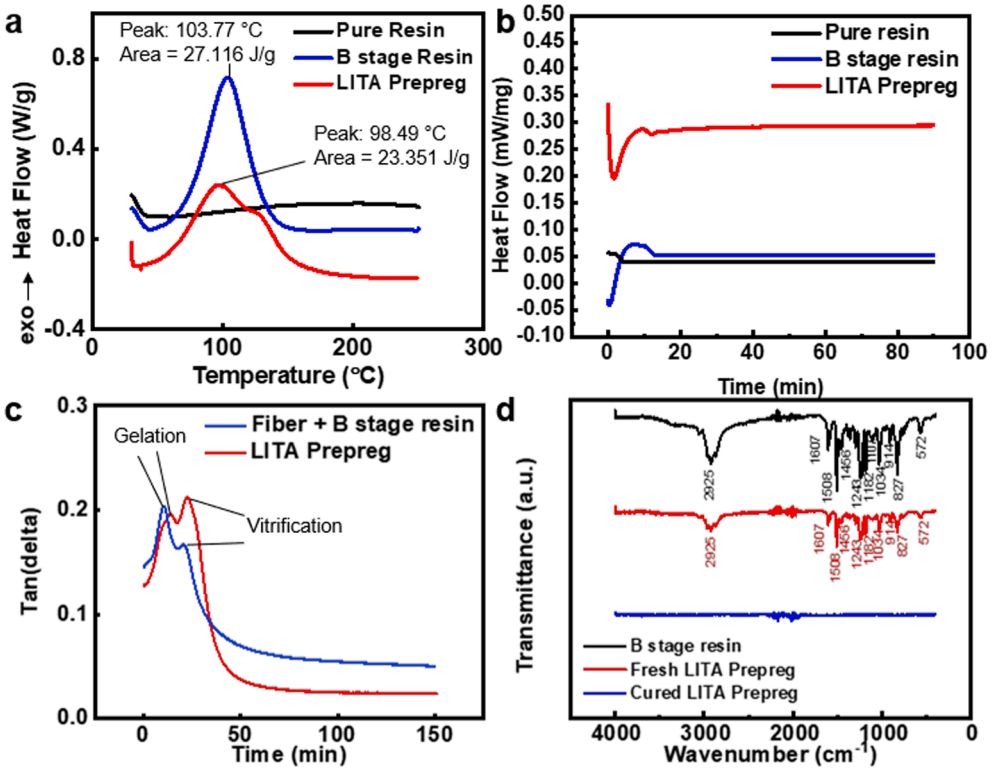

Fig. 7. B stage confirmation of the LITA prepregs. (a) Differential scanning calorimetry (DSC) profile of resin, B stage resin, and the LITA prepreg (measured from 30 to 250 °C, heat ramp rate 5 °C/min). (b) Isothermal DSC isothermal profile of resin, B stage resin, and the LITA prepreg tested at 30 °C for 90 min. (c) Dynamic mechanical analysis (DMA) isothermal profile of the fiber that absorbs B stage resin, and the LITA prepreg at 80 °C for 150 min (1 Hz). (d) Fourier transform infrared spectroscopy (FTIR) profile of B stage resin, fresh and cured LITA prepreg. (For interpretation of the references to colour in this figure legend, the reader is referred to the web version of this article.)

the right edge of the heater. With heating applied, it took the resin 80 s to infiltrate, while it did not infiltrate by 600 s without heat. Fig. 6(h) shows the continuous wicking of polyester resin on woven fabrics with heating applied. Therefore, the woven fabrics are proven the capability of using the LITA method.

B-stage is the partial crosslinking status in the system where resin is mixed with hardener.[29,30] The B-stage of the LITA prepregs is confirmed by characterizing degree of curing, crystallization peaks,

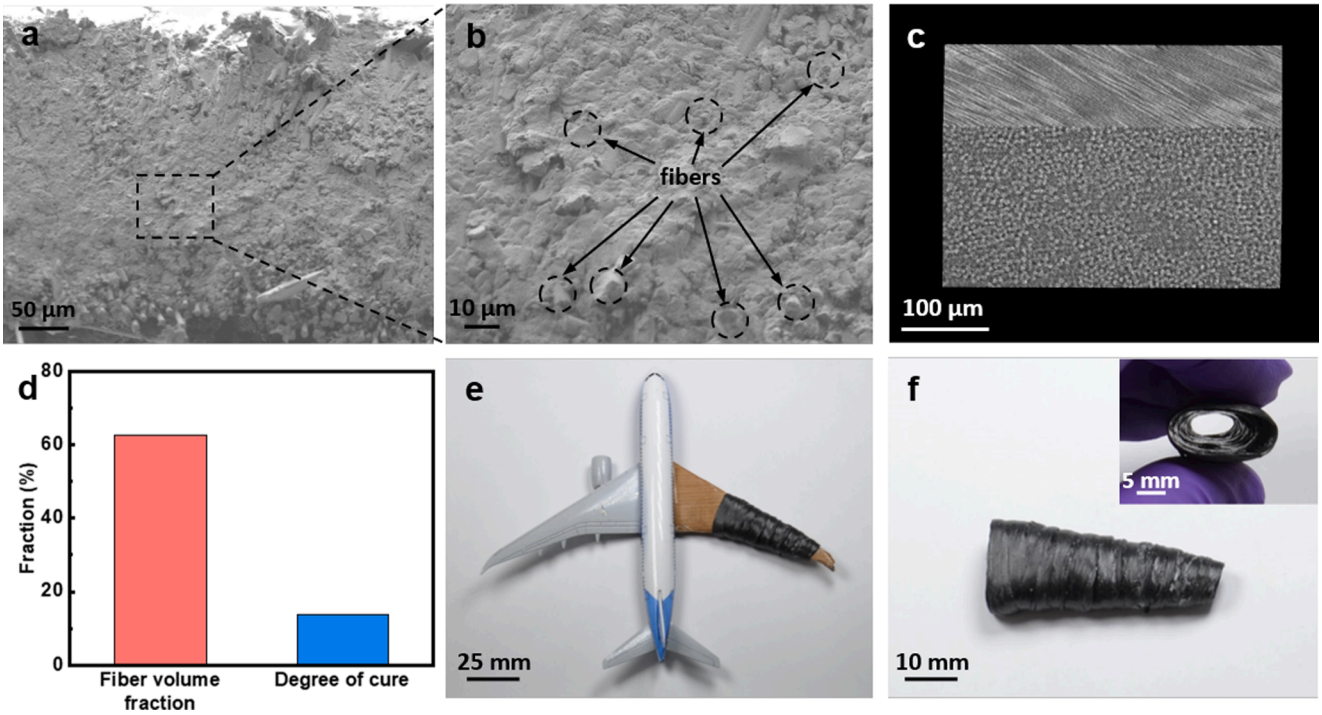

Fig. 8. Morphology characterization and wing composite demonstration. (a) Cross-sectional Scanning electron microscopy (SEM) image of the LITA prepreg. (b) Enlarged cross-sectional SEM image of the LITA prepreg, with fibers covered with thermoset resin matrix. (c) Nano-computed tomography (nano-CT) reconstructed image of the cross-section of the prepreg, showing fiber is infiltrated with resin. (d) Column plot that shows fiber volume fraction and degree of cure. (e) Digital photos of the LITA prepreg that is laid up on the wing of the small-scale aircraft model. (f) The surface and the cross-sectional views of the prepreg after it is fully cured. (For interpretation of the references to colour in this figure legend, the reader is referred to the web version of this article.)

gelation and vitrification points, and functional groups, and comparing them with pure resin, B-stage resin, and carbon fiber wetted with B-stage resin. The differential scanning calorimetry (DSC) profile tested on Q600 (TA Instruments) and Discovery DSC (TA Instruments) characterizes the exothermic peaks of the fresh B-stage resin and the fabricated prepreg occur at 103.77 °C and 98.49 °C, respectively (Fig. 7(a)). No significant exothermic peak occurs in the differential scanning calorimetry (DSC) curve of the pure resin, indicating that the crosslinking does not occur in resin without a hardener. The B-stage resin needs residual heat of reaction as 27.116 J/g to fully cure, while the prepreg needs 23.351 J/g to fully cure. The degree of cure of the prepreg can be calculated as 13.9% from the residual heat of reaction. The low degree of cure confirms the LITA prepreg is at the B stage, indicating that it is far from being fully cured. The isothermal DSC test was utilized to characterize endothermic peaks for 90 min on Q600 (TA Instruments) (Fig. 7(b)). For the pure resin, there is no endothermic peak in its isothermal profile, but there is one for the B-stage resin and the LITA prepreg respectively on the early test minutes (in ~ 0.5 min for B-stage resin, and in ~ 2 min for the prepreg), followed by slight exothermic signals (in ~ 7 min for B-stage resin, and in ~ 10 min for the prepreg). Those endothermic peaks indicate that their molecular mobility slightly increased due to rapid temperature increase from room temperature in the beginning. The subsequent exothermic signals suggest that they underwent crystallization due to crosslinking, but did not have high heat flow due to low temperature testing conditions.[31] It confirms the LITA prepreg was at B-stage before testing. The dynamic mechanical analysis (DMA) results using DMA Q800 (TA Instruments) in Fig. 7(c) isothermally characterized tan(delta) (the ratio of loss modulus to storage modulus) values at 80 °C for 150 min (1 Hz) for both the fiber that absorbs B-stage resin and the LITA prepreg. The tan(delta) appears first peak in ~ 10 min for the fiber wetted with resin, and in ~ 13 min for the LITA prepreg. The first peak can be interpreted as the gelation, where the materials transitioned from viscous liquid to rubbery solid, due to increasing viscosity during gel formation. Then the curve increases to form the second peak, which appears in ~ 21 min for the fiber wetted with resin, and in 22 min for the LITA prepreg. The formation of the second peak can be construed as the transition from rubbery solid to glass. After the second peak, both the tan(delta) curves dramatically decrease, which reveals that storage modulus is at least one order of magnitude higher than loss modulus and embodies the solid-like behaviors, so the second peak is the vitrification. The curves prove that both the fibers wetted with resin and the LITA prepreg were before the gelation stage in the beginning of DMA test, so they were in the B stage. The normalized Fourier transform infrared (FTIR) spectroscopy profiles (Fig. 7(d)) show that in the B-stage resin, several functional groups can be identified from transmittance peaks, such as the epoxy group (914 and 1243 cm^{-1}), the C-O group (1034 and 1107 cm^{-1}), the phenyl group (827 and 1182 cm^{-1}), the methyl group (1456 and 2925 cm^{-1}), the C = C bond from the aromatic ring (1508 and 1607 cm^{-1}).[32,33] Those transmittance peaks decrease in the fresh LITA prepreg but are still observable. The fully cured prepreg does not show obvious transmittance peaks compared to the previous two FTIR spectra, indicating that the functional groups of the resin matrix have all reacted to the curing. The observability of the transmittance bands in the FTIR spectra of the fresh LITA prepreg can confirm that the fresh prepreg is at the B stage. All the DSC temperature ramp test, isothermal test, DMA and FTIR tests have confirmed the B-staging status of the prepreg. [34,35]

The morphology and the application demonstration of the prepregs are shown in Fig. 8. As shown in SEM images in Fig. 8(a), it can be observed in the cured LITA prepregs that the majority of the volumes are covered by the thermoset resin matrix in the cross-sectional area, and the high magnification SEM image in Fig. 8(b) shows clearly the resin coverage on multiple spots on the cross-section of the fiber. The Nano-CT scanned 3D model, which has an as high resolution as 325 μm, is able to exhibit carbon fibers whose diameter is 5.2 μm (HexTow, Hexcel Corporation, Stamford, CT). The model shows that the resin is filled in the spaces between fibers in the cross-sectional area in Fig. 8(b). The column plot in Fig. 8(c) shows the fiber volume fraction of the prepreg is approximately 62.8 % by measuring the prepreg density using Archimedes' method and calculating fiber volume fraction in Rule of Mixture equation of density, and the degree of cure is 13.9% from the DSC temperature-dependent profile. Fig. 8(d) shows that the LITA prepreg was laid upon the wing of the small-scale aircraft model to demonstrate the moldability, making the external profiles of the prepreg similar to those of the wing. After the prepreg was fully cured on the wing, the prepreg was taken out with a hollow structure created, showing the cured prepreg was conformable to the wing geometrically (Fig. 8(e)). When the prepreg was fully cured, the rigidity of the composites structure could ensure that the hollow structure retained the shape fidelity. This demonstration proves that our prepreg is easily moldable and conformable to complex geometry, and can be applied in load-bearing structures.

Table 1
Key parameters used for estimation of the scaled-up LITA prepreg fabrication.

Parameters	Value
Infusion time/s	24
Power output/W	6.68
Fiber tow width/mm	2.50
Weight per 10 mm-long tow/(g)	0.011

Table 2
Production rate of conventional production methods.

Production Methods	Production Rate (ft/hr)	Ref.
Resin Filming Prepreg Method	750	[23]
Hot Melt Prepreg Method	295.28	[24]

Table 3
Energy intensity of conventional production methods.

Production Methods	Energy Intensity (MJ/kg)	Ref.
Traditional Prepreg Method	40	[27,28]
Spray Up	14.9	[27,28]
Resin Transfer Molding	12.8	[27,28]
Vacuum Assisted Resin Fusion	10.2	[27,28]

Table 1 lists key parameters used for scaling up the production, used from Fig. 2(d). The wicking experiment obtains 4 s as the wicking time (frequency of laboratory-scale dispensing as 0.2 Hz) and 24 s as the infusion time to infiltrate the 10-mm region, using the power output 6.68 W. In the scaling-up application, a 10-Hz inkjet box is assumed as the resin container and the droplet feeder, then the production speed can be increased by 50 times than the laboratory-scale operation, and obtain the average production speed as 688.82 ft/hr (209.95 m/hr). The speed allows the occurrence of resin wicking and resin impregnation into the fiber, with continuous and frequency-controlled resin droplets to produce the well-infiltrated and well amount-controlled prepregs. The production speed is 133.28% higher than the hot-melt prepreg method. Theoretically, the frequency can be selected as a higher one for the inkjet box, which provides a larger amount of resin feeding and accelerates the production, but the corresponding production speed of our selected inkjet frequency can already rival other prepreg fabrication methods. The energy intensity of our method is estimated as 14.575 MJ/kg. The estimation is shown in equations (1) and (2), utilizing the corresponding key parameters from Table 1. The production rate and the energy intensity of conventional prepreg production methods are listed in Table 2 and 3. Fig. 9 shows the production speed and the energy density of our LITA prepreg fabrication method by comparing it with other conventional prepreg fabrication methods.

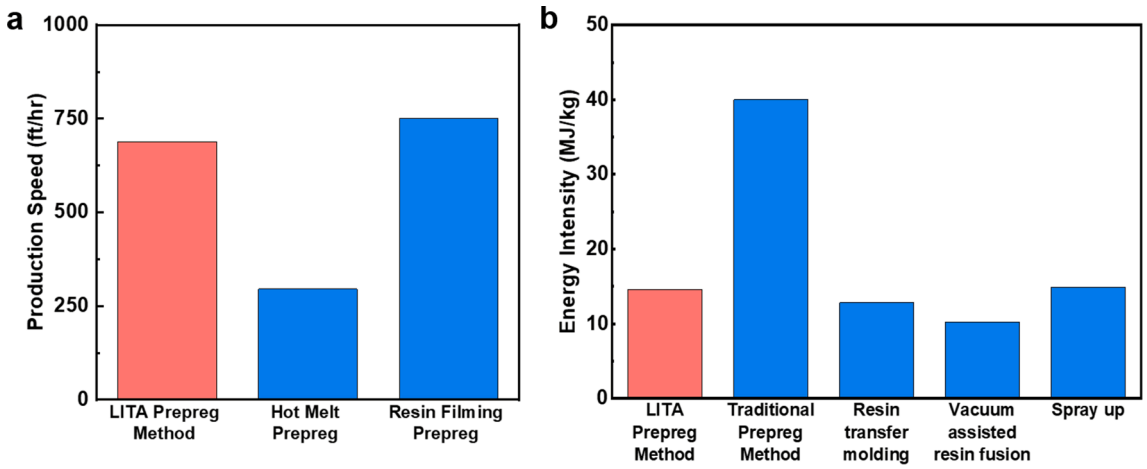

Fig. 9. Production rate and energy intensity of LITA prepreg method compared with other production methods. (a) Comparison of production rate with other conventional prepreg fabrication methods (data adapted from [23–26], using average values of the given data range). (b) Comparison of energy intensity with the traditional prepreg production method and other production methods. (data adapted from [27,28]). (For interpretation of the references to colour in this figure legend, the reader is referred to the web version of this article.)

$$Energy = Power\ output * Infusion\ time = 6.68 * 24 = 160.32J \quad (1)$$

$$Energy\ Intensity = 160.32/0.011 = 14574.55J/g \approx 14.575MJ/kg \quad (2)$$

In comparison with the data from [27,28], the energy intensity of our method is 63.56% lower than the traditional prepreg fabrication methods. The high production speed and the low energy intensity embodies the competitiveness of our LITA prepreg method.

2. Conclusion

Our LITA thermoset prepreg fabrication method exhibits its advantages over other methods by ensuring the adequacy of impregnation, eliminating the solvents, expanding the material selection for thermoset resins and reducing energy consumption at the same time. In our bench-scale continuous prepregs production system, the capillary effect is induced by the adjacent heater to realize the fast resin wicking on carbon fibers, which can be achieved within 5 s. The heater controls the resin viscosity by creating a temperature gradient on the fiber, drives the resin flow front towards the heater location, and also the gravity factor brought by the slope helps resin flowing. The initial viscosity of resin plays an important role in the LITA method. With low viscosity, the resin can flow along the LITA conveyor solely by gravity. With heating applied, the viscosity can decrease so that it flows more easily due to capillary force as well as gravity. Too high initial viscosity would impede the resin ability to decrease viscosity to the flowable range. We have tested the epoxy resin and the polyester resin in the LITA method. The viscosity of the epoxy resin is 4 Pa·s at 30 °C, and the initial viscosity of the polyester resin is 0.713 Pa·s at 25 °C. Both resin systems work in our LITA method. The applicable viscosity range can be determined as 0.713 ~ 4 Pa·s at room temperature. The rise of heater temperature can lead to the increase of the spectrum of temperature gradient, which creates a variety of viscosity values of resin on fibers. To further improve the resin impregnation rate, the heater temperature should be further increased to create a smooth transition in the temperature gradient, which can drive the resin flow front with low viscosity at the elevated temperature. The resulting prepreg possesses degree of curing as 13.9%, confirming its B-staging. The scaled-up LITA prepreg fabrication process can consume 63.56% lower energy than the traditional prepreg fabrication methods, and achieve higher production rate by 133.28% than the traditional hot-melt prepreg method. The LITA prepreg fabrication technology offers an efficient and eco-friendly composite manufacturing strategy due to its fast production speed and low energy costs, which stands out from other energy-intensive prepreg fabrication methods. We have to mention that it is the capital cost that dominates the processing methods. The motivation of our current work is to propose a new strategy to fabricate prepregs as an eco-friendlier alternative to existing energy-intensive counterpart.

CRediT authorship contribution statement

Kaiyue Deng: Writing – original draft, Investigation, Writing – review & editing. **Chunyan Zhang:** Writing – review & editing. **Xiangyang Dong:** Formal analysis, Data curation. **Kun Kelvin Fu:** Conceptualization, Supervision.

Declaration of Competing Interest

The authors declare that they have no known competing financial interests or personal relationships that could have appeared to influence the work reported in this paper.

Acknowledgments

The authors would like to appreciate the funding support from the University of Delaware startup. X.D. also gratefully acknowledges partial support provided by AFOSR grant FA9550-21-1-0226.

References

[1] Centea T, Grunenfelder LK, Nutt SR. A review of out-of-autoclave prepregs – Material properties, process phenomena, and manufacturing considerations. Compos Part A Appl Sci Manuf 2015;70:132–54. https://doi.org/10.1016/j.compositesa.2014.09.029.
[2] Lee JM, Kim BM, Ko DC. Development of vacuum-assisted prepreg compression molding for production of automotive roof panels. Compos Struct 2019;213:144–52. https://doi.org/10.1016/j.compstruct.2019.01.092.
[3] Robert C, Pecur T, Maguire JM, Lafferty AD, McCarthy ED, Brádaigh CMÓ. A novel powder-epoxy towpregging line for wind and tidal turbine blades. Compos Part B Eng 2020;203:108443. https://doi.org/10.1016/j.compositesb.2020.108443.
[4] Stewart AL, Poursartip A. Characterization of fibre alignment in as-received aerospace grade unidirectional prepreg. Compos Part A Appl Sci Manuf 2018;112:239–49. https://doi.org/10.1016/j.compositesa.2018.04.018.
[5] Wulfsberg J, Herrmann A, Ziegmann G, Lonsdorfer G, Stöß N, Fette M. Combination of Carbon Fibre Sheet Moulding Compound and Prepreg Compression Moulding in Aerospace Industry. Procedia Eng 2014;81:1601–7. https://doi.org/10.1016/j.proeng.2014.10.197.
[6] Michaud V, Sequeira Tavares S, Sigg A, Lavanchy S, Manson J-AE. Low Pressure Processing of High Fiber Content Composites. 8th Int. Conf. Flow Process. Compos. Mater., Douai, France: 2006, p. 393–400.
[7] Bao J, Shi Y, Xie C, Fantuzzi N, Hu D, Arikan MH, et al. A Systematic Characterization Approach for Vacuum Bag Only Prepregs towards an Accurate

Process Design. Materials (Basel) 2022;15:451. https://doi.org/10.3390/MA15020451.
[8] Yizhi Guo. Fibers Microbuckling of Uncured Carbon-Epoxy Prepreg in Bending. Oregon State University; 2017.
[9] Ersoy N, Garstka T, Potter K, Wisnom MR, Porter D, Clegg M, et al. Development of the properties of a carbon fibre reinforced thermosetting composite through cure. Compos Part A Appl Sci Manuf 2010;41:401–9. https://doi.org/10.1016/J.COMPOSITESA.2009.11.007.
[10] Belnoue JP-H, Mesogitis T, Nixon-Pearson OJ, Kratz J, Ivanov DS, Partridge IK, et al. Understanding and predicting defect formation in automated fibre placement pre-preg laminates. Compos Part A Appl Sci Manuf 2017;102:196–206. https://doi.org/https://doi.org/10.1016/j.compositesa.2017.08.008.
[11] United Nations. Global Roadmap for Accelerated SDG7 Action. 2021.
[12] International Energy Agency (IEA). Net Zero by 2050 – A Roadmap for the Global Energy Sector 2021. https://www.iea.org/reports/net-zero-by-2050 (accessed April 13, 2022).
[13] Intergovernmental Panel on Climate Change (IPCC). Special Report - Global Warming of 1.5 °C n.d. https://www.ipcc.ch/sr15/ (accessed April 13, 2022).
[14] Shin JH, Jang HK, Choi WH, Song TH, Kim CG, Lee WY. Design and verification of a single slab RAS through mass production of glass/MWNT added epoxy composite prepreg. J Appl Polym Sci 2015;132:42019. https://doi.org/10.1002/APP.42019.
[15] Wang R-M, Zheng S-R, Zheng Y-P. Fabrication of the half-finished products for polymer composites. Polym Matrix Compos Technol 2011:213–548. https://doi.org/10.1533/9780857092229.2.213.
[16] Cender TA, Simacek P, Advani SG. Resin film impregnation in fabric prepregs with dual length scale permeability. Compos Part A Appl Sci Manuf 2013;53:118–28. https://doi.org/10.1016/J.COMPOSITESA.2013.05.013.
[17] Hanaoka T, Ikematsu H, Takahashi S, Ito N, Ijuin N, Kawada H, et al. Recovery of carbon fiber from prepreg using nitric acid and evaluation of recycled CFRP. Compos Part B Eng 2022;231:109560. https://doi.org/10.1016/j.compositesb.2021.109560.
[18] Hayes BS, Seferis JC, Edwards RR. Self-adhesive honeycomb prepreg systems for secondary structural applications. Polym Compos 1998;19:54–64. https://doi.org/10.1002/pc.10075.
[19] Vashisth A, Healey RE, Pospisil MJ, Oh JH, Green MJ. Continuous processing of pre-pregs using radio frequency heating. Compos Sci Technol 2020;195:108211. https://doi.org/10.1016/j.compscitech.2020.108211.
[20] Miaris A, Päßler M, Lichtner J, Schledjewski R. "Siphon impregnation": The development of a new method for impregnation during filament winding. ICCM Int. Conf. Compos. Mater. 2009.
[21] Better impregnation of prepregs thanks to T-Die method | Plastics n.d. https://www.plastics.gl/automotive/better-impregnation-of-prepregs-thanks-to-t-die-method/ (accessed March 30, 2022).
[22] Shi B, Shang Y, Zhang P, Cuadros AP, Qu J, Sun B, et al. Dynamic Capillary-Driven Additive Manufacturing of Continuous Carbon Fiber Composite. Matter 2020;2:1594–604. https://doi.org/10.1016/J.MATT.2020.04.010.
[23] Campbell FC. Structural Composite Materials. ASM. International 2010.
[24] Edie DD, Lickfield GC, Drews MJ, Ellison L E Allen MS, McCollum JR, Thomas HL. Thermoplastic Coating of Carbon Fibers. NASA Annu Rep 1988.
[25] Lukaszewicz DHJA, Ward C, Potter KD. The engineering aspects of automated prepreg layup: History, present and future. Compos Part B Eng 2012;43:997–1009. https://doi.org/10.1016/J.COMPOSITESB.2011.12.003.
[26] Andrianov A, Tomita EK, Veras CAG, Telles B. A Low-Cost Filament Winding Technology for University Laboratories and Startups. Polymers (Basel) 2022;14:1066. https://doi.org/10.3390/POLYM14051066.
[27] Song YS, Youn JR, Gutowski TG. Life cycle energy analysis of fiber-reinforced composites. Compos Part A Appl Sci Manuf 2009;40:1257–65. https://doi.org/10.1016/J.COMPOSITESA.2009.05.020.
[28] Suzuki T, Takahashi J. Prediction of Energy Intensity of Carbon Fiber Reinforced Plastics for Mass-Produced Passenger Cars. Ninth Japan Int. SAMPE Symp. 2005:14–9.
[29] Kim WG, Kim HS. B-Stage Characterization of o-Cresol Novolac Epoxy Resin System Using Raman Spectroscopy and Matrix-Assisted Laser Desorption/Ionization Mass Spectrometry. J Appl Polym Sci 2000;76:1940–6. https://doi.org/10.1002/(SICI)1097-4628(20000624)76:13.
[30] Studer J, Dransfeld C, Masania K. An analytical model for B-stage joining and co-curing of carbon fibre epoxy composites. Compos Part A Appl Sci Manuf 2016;87:282–9. https://doi.org/10.1016/J.COMPOSITESA.2016.05.009.
[31] Keller A, Masania K, Taylor AC, Dransfeld C. Fast-curing epoxy polymers with silica nanoparticles: properties and rheo-kinetic modelling. J Mater Sci 2016;51:236–51. https://doi.org/10.1007/s10853-015-9158-y.
[32] dos Santos AS, de Oliveira TC, Rodrigues KF, Silva AAC, Coppio GJL, da Silva Fonseca BC, et al. Amino-functionalized carbon nanotubes for effectively improving the mechanical properties of pre-impregnated epoxy resin/carbon fiber. J Appl Polym Sci 2021;138:51355. https://doi.org/10.1002/app.51355.
[33] Sales RCM, Diniz MF, Dutra RCL, Thim GP, Dibbern-Brunelli D. Thermal curing of glass-epoxy prepregs by luminescence spectroscopy. J Appl Polym Sci 2010;117:664–71. https://doi.org/10.1002/app.31953.
[34] Ganapathi AS, Joshi SC, Chen Z. Influence of cure kinetic, rheological and thermo-mechanical behavior on micro-level curing strain of an epoxy prepreg. J Therm Anal Calorim 2016;124:305–16. https://doi.org/10.1007/s10973-015-5090-2.
[35] Zhang Z, Beatty E, Wong CP. Study on the Curing Process and the Gelation of Epoxy/Anhydride System for No-Flow Underfill for Flip-Chip Applications. Macromol Mater Eng 2003;288:365–71. https://doi.org/10.1002/mame.200390029.